Macromolecules
ARTICLE

Macromolecules **2009**, *42*, 4739–4745 **4739**
DOI: 10.1021/ma900004d

Effect of Polylactide Stereocomplex on the Crystallization Behavior of Poly(L-lactic acid)

Nelly Rahman,[†] Takahiko Kawai,*[,‡] Go Matsuba,[†] Koji Nishida,[†] Toshiji Kanaya,[†] Hiroshi Watanabe,[†] Hirotaka Okamoto,[§] Makoto Kato,[§] Arimitsu Usuki,[§] Masatoshi Matsuda,[⊥] Katsuhiko Nakajima,[⊥] and Nobutaka Honma[⊥]

[†]*Institute for Chemical Research, Kyoto University, Uji, Kyoto 611-0011, Japan,* [‡]*Graduate School of Engineering, Gunma University, Ota, Gunma 373-0057, Japan,* [§]*Toyota Central R&D Labs Inc., Nagakute, Aichi 480-1192, Japan, and* [⊥]*Toyota Motor Corporation, Toyota, Aichi 410-1193, Japan*

Received January 4, 2009; Revised Manuscript Received April 19, 2009

ABSTRACT: Effects of the addition of PDLA on the crystallization behavior of PLLA was investigated by means of differential scanning calorimetry, wide-angle X-ray diffraction, melt rheology, and polarized optical microscopy. Nonisothermal and isothermal crystallization behavior of PLLA including low (*l*-PDLA) and high molecular weight PDLA (*h*-PDLA) were studied. PLLA/PDLA asymmetric blends form stereocomplex (SC) crystal and stay unmelted at 200 °C in the PLLA melt. Nonisothermal crystallization measurement from 200 °C showed monotonous rise in the crystallization temperature for PLLA/*h*-PDLA blend, while peculiar concentration dependence was observed for PLLA/*l*-PDLA blends. The acceleration effect was more pronounced in PLLA/*h*-PDLA, although the crystallinity of SC was lower than PLLA/*l*-PDLA blends, which implies the importance of higher order structure of SC for the crystallization of PLLA. From isothermal crystallization kinetics measurements, the acceleration effect in PLLA/*h*- and *l*-PDLA blends was found to enhance the nucleation of crystallization but slightly interrupts the crystallization growth. The above results were reasonably explained by the model where SC crystallites are not isolated in PLLA melt but connected like a physical gel.

1. Introduction

Recently, several factors such as soaring oil prices, worldwide interest in renewable resources, growing concern regarding greenhouse gas emission, and a new emphasis on waste management have created renewed interest in biopolymers and the efficiency with which they can be produced. Poly(L-lactic acid), PLLA, is one of the most promising candidates because it is completely derived from renewable resources such as corn, potato starch, cane, cheese whey, etc. It contributes not only to decreasing oil consumption but also to the prevention of global warming because it originates from plants which absorb carbon dioxide in the atmosphere. PLLA is a thermoplastic, high-strength, high-modulus polymer for use in either the industrial packaging field or the biocompatible/bioabsorbable medical device market. It is easily processed on standard plastics equipment to yield molded parts, film, or fibers.[1] However, PLLA has very bad processability because of slow crystallization rate under supercooled state.[2]

It has been reported that PLLA crystallizes into various crystalline forms. Three crystalline forms (α, β, and γ) have been reported for PLLA. Crystallization from the melt or from solution leads to α form crystal, which is most common polymorph.[3−8] In α form, it is considered that two chains with 10_3 helical conformation are packed into an orthorhombic unit cell with dimension of a = 10.7 Å, b = 6.45 Å, and c(fiber axis) = 27.8 Å.[6] We have recently investigated that the crystal structure of α-form slightly varies when PLLA is crystallized below 120 °C, and the lattice parameters stay constant below 90 °C. It is concluded that ordered type α-form is obtained above 120 °C, while disordered type α′-form crystallizes below 90 °C.

*Corresponding author: e-mail: kawai@eng.gunma-u.ac.jp; tel: +81-276-50-2435; fax: +81-276-50-2435.

The second phase, β form, is obtained under high drawing conditions and high temperatures.[5,9] According to the recent study by Puggiani et al., the β form is considered to have a frustrated structure, containing three chains in a trigonal unit cell with $a = b$ = 10.52 Å and c = 8.8 Å.[10] Recently, Cartier et al. have reported that a third crystal modification of PLLA, γ form, was obtained via epitaxial crystallization on hexamethylbenzene substrate.[9] It has two antiparallel 3_1 helices packed in an orthorhombic unit cell with a = 9.95 Å, b = 6.25 Å, and c = 8.8 Å.

In addition to the polymorphous of PLA homopolymer, the formation of a stereocomplex (SC) by blending enantiomeric PLLA and PDLA was extensively studied during the past decade.[11−15] A stereocomplex racemic crystallite having a 3_1 helical structure is different from a homopolymer crystallite with a 10_3 helical structure found in α-form of individual PLLA or PDLA.[16] The unit cell of SC crystal was recently reported by Sawai et al. to be a trigonal cell with cell constants of $a = b$ = 1.50 nm, c = 0.823 nm, α = β = 90°, and γ = 120°.[17] More compact side-by-side crystallization between the two enantiomeric polymers results in a much higher melting point. The melting point of SC has been reported to be around 230 °C, which is ∼50 °C higher than that of either lactide homopolymer.[11−15]

Enhancement of overall crystallization rate of PLLA is a matter of concern when PLLA is utilized for various industrial applications. Numerous studies have been carried out for improving the crystallization rate of PLLA by mixing with nucleating agent such as talc.[18,19] Besides study on addition of an inorganic nucleating agent to enhance crystallization rate of PLLA, it also reported that crystallization rate of PLLA increased with addition of poly(D-lactic acid), PDLA.[20]

When the asymmetric blend of PLLA and PDLA is subjected to heat up to 200 °C, all the homocrystals are in the molten state

Published on Web 06/09/2009

while the SC crytallites stay unmelted because of its high melting temperature.[20−23] Intensive studies mainly on the crystallization kinetics have been performed by means of calorimetry.[24−33] Schmidt et al. pointed out that the SC crystal acts as a nucleating agent. However, the crystallization behavior of PLLA seems not to have been examined sufficiently in those publications.

Our interests mainly focus on whether the SC crystal accelerates the crystallization of PLLA by the simple "nucleating agent model", which the epitaxial relationship between the crystal lattice of nucleating agent and that of polymer plays an important role. Considering that the SC crystal has a different chain conformation as described above, i.e., different surface topology from that of a-form of PLLA, the nucleating agent model should be discussed in more detail. The aim of this report is to clarify the mechanism of PLLA crystallization under existence of stereocomplex. We are going to show in this study the peculiar PDLA concentration dependence of PLLA crystallization, which might arise from the condition for the formation of SC crystallites. The mechanism for the acceleration of PLLA crystallization is discussed on the basis of the detailed analysis of the SC structure in the molten state of PLLA as well as isothermal crystallization kinetics.

2. Experimental Section

2.1. Materials and Sample Preparation. PLLA, low molecular weight PDLA (*l*-PDLA), and high molecular weight PDLA (*h*-PDLA) were supplied by Toyota Motor Corp. The weight-average molecular weights of the samples are 215 000, 30 800, and 228 000 for PLLA, *l*-PDLA, and *h*-PDLA, respectively. PLLA and PDLA were dissolved in chloroform and stirred for 1 h. The solution was cast onto flat dishes, and then the solvent was allowed to evaporate at room temperature for ~1 day. The obtained cast films were dried in vacuum drier at 70 °C for 4 h. The dried cast films were pressed in the hot press at 240 °C for 2 min and then quenched into ice water in order to obtain amorphous films. The samples were then isothermally crystallized at 100 °C for 30 min to allow SC and PLLA homopolymer to crystallize prior to melt at 200 °C for 2 min. Various thermal histories, after precrystallization process at 100 °C and melting at 200 °C, were applied to the samples according to the measurement. For differential scanning calorimetry, the samples were cooled to room temperature with a cooling rate of 2.5 °C/min to follow the nonisothermal crystallization behavior. While for polarized optical microscopy, the samples were isothermally crystallized at 140 °C to follow the crystallization behavior of PLLA/PDLA blends. The blends quenched from 200 °C were subjected to wide-angle X-ray analysis.

2.2. Measurements. Nonisothermal crystallization behavior of the samples was analyzed with a differential scanning calorimeter (DSC), Perkin-Elmer Diamond DSC, which was calibrated by the melting of indium and tin. The DSC scans were carried out in a flowing-nitrogen atmosphere. Wide-angle X-ray diffraction (WAXD) measurement was carried out at room temperature using a Rigaku RINT-2000 diffractometer for PLLA/PDLA blends quenched from 200 °C. A monochromatized Cu Kα radiation ($\lambda = 0.154$ nm) was transmitted through the sample. Dynamic viscoelasticity measurements were carried out at 200 °C under a N_2 atmosphere by using stress rheometer ARES (Rheometrics Co. Ltd.; currently TA) for PLLA/PDLA blends with various PDLA concentration. Time evolution of spherulite growth in the film was recorded under crossed polars with Nikon Optiphot2-Pol with a charged coupling device camera equipped with a Mettler FP82HT hot stage.

3. Results and Discussion

3.1. Nonisothermal Crystallization Behavior. In order to estimate the effect of PDLA concentration and/or molecular weight, nonisothermal crystallization measurements were carried out by means of differential scanning calorimetry (DSC). The amorphous films of PLLA/PDLA blend were first precrystallized at 100 °C for 30 min prior to the melt crystallization to obtain the same thermal history for each PLLA/PDLA blend. Thirty minutes at 100 °C was long enough to complete the crystallization of each blend and molecular weight of PDLA. The precrystallized PLLA/PDLA blends were then heated up to 200 at 10 °C/min and kept for 2 min before cooling crystallization with a constant cooling rate of 2.5 °C/min.

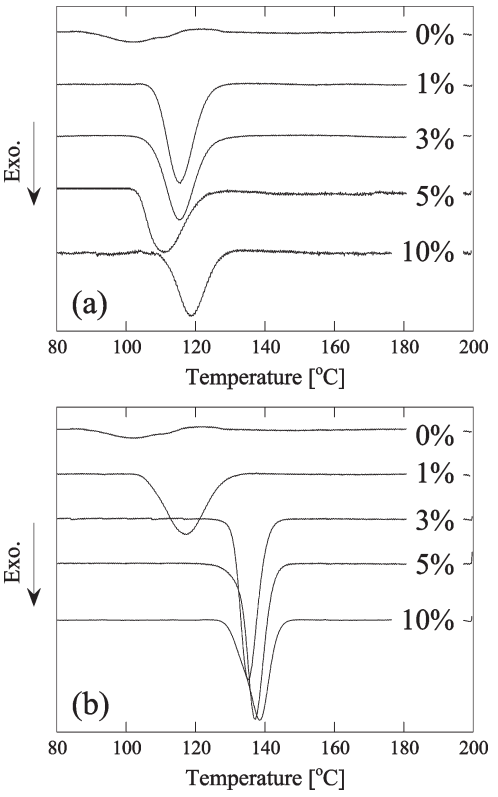

Figure 1. DSC thermograms of PLLA with various concentrations of *l*-PDLA (a) and *h*-PDLA (b) during cooling from 200 °C. The samples were precrystallized at 100 °C prior to the melt.

Figure 1 shows the DSC traces obtained during cooling process of (a) PLLA/*l*-PDLA blends and (b) PLLA/*h*-PDLA blends. Since stereocomplex (SC) crystal stays unmelted at 200 °C, the exothermic peak indicates the crystallization of PLLA and/or PDLA homocrystal as reported by several authors.[20−24,32] As one can see clearly for PLLA/*h*-PDLA blends, the crystallization temperature, T_c, rises with increasing *h*-PDLA concentration. The crystallization temperature of PLLA/*h*-PDLA 3% is ca. 30 °C higher than that of PLLA homopolymer (0%). The crystallization exothermic peak tends to be larger with increasing *h*-PDLA concentration, suggesting the remarkable increase in crystallinity. The above finding strongly indicates the existence of SC crystal accelerates the crystallization of PLLA. Interestingly, a peculiar PDLA concentration dependence was seen in PLLA/*l*-PDLA blends (Figure 1a). The crystallization temperature does not change monotonously with *l*-PDLA concentration.

A different PDLA concentration effect on PLLA crystallization according to the molecular weight of PDLA is more clearly shown in Figure 2, where the T_c during cooling is plotted against both *l*-PDLA and *h*-PDLA concentrations. For *h*-PDLA blends, T_c rises with increasing *h*-PDLA concentration as mentioned above, while *l*-PDLA blends show peculiar concentration dependence. The T_c shows a steep rise

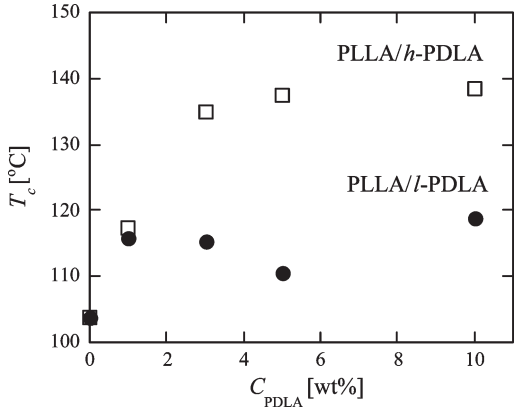

Figure 2. Plots of the crystallization temperature, T_c, of PLLA/PDLA blends during cooling as a functions of PDLA concentration. The samples were precrystallized at 100 °C prior to the melt at 200 °C.

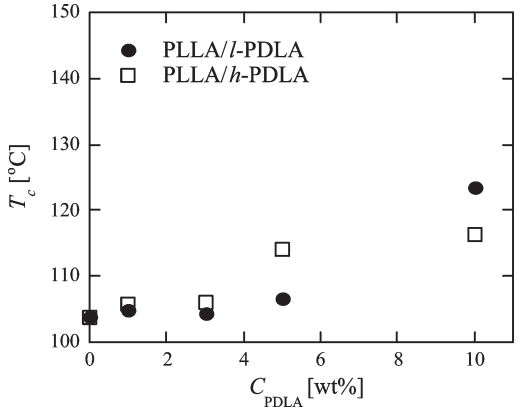

Figure 3. Plots of the crystallization temperature, T_c, of PLLA/PDLA cast blends during cooling as a functions of PDLA concentration.

up to 1%, followed by leveling off with increasing concentration in *l*-PDLA blends. Among the publications regarding with the crystallization acceleration effect of SC, this unique concentration dependence seen in PLLA/*l*-PDLA blends has not been reported. Yamane and Sasai reported the monotonous rise in crystallization temperature when the solvent cast film was melted at 200 °C, followed by slow cooling at 2 °C/min.[21] The molecular weight of PDLA does affect the overall crystallization rate of PLLA, while the monotonous rise in crystallization temperature are seen for all the sample with various molecular weight of PDLA. The discrepancy between our results in Figure 2 and that published by Yamane et al.[21] may be attributed partly to the differences in PLLA and PDLA samples such as molecular weight, molecular weight distribution, optical purity, and so on. However, it should be pointed out that the thermal history applied for SC formation is different in our study.

In order to clarify the origin of the peculiar concentration dependence in PLLA/*l*-PDLA blends, cast film was directly used for the measurement for comparison. The cast films with various PDLA concentrations were heated up to 200 °C without further precrystallization procedure, followed by cooling with the rate of 2.5 °C/min. In this procedure, it is supposed that the SC formation takes place during the evaporation of chloroform. Figure 3 shows the PDLA concentration dependence on the crystallization temperature, T_c, for cast films. The crystallization temperature rises with increasing PDLA concentration. This concentration dependence seems to be independent of molecular weight of PDLA, since there is no clear distinction in T_c between

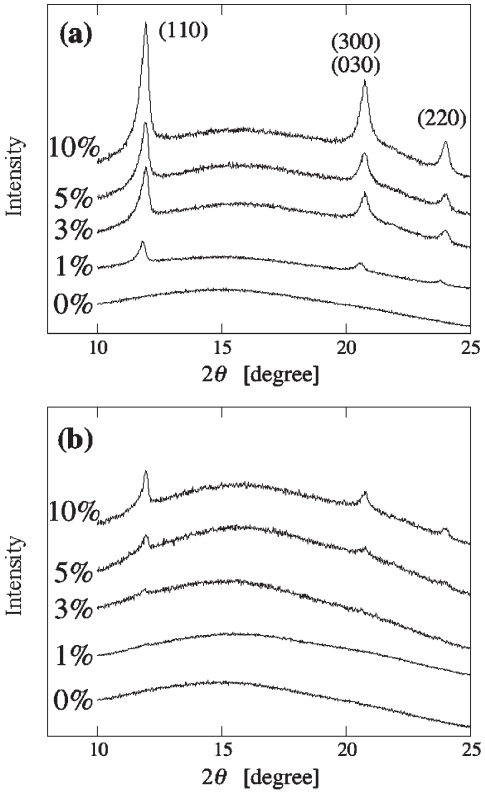

Figure 4. WAXD profiles of melt quenched PLLA with various concentrations of *l*-PDLA (a) and *h*-PDLA (b).

h- and *l*-PDLA blends. In addition to the monotonous concentration dependence in T_cs, it should be pointed out that the precrystallized film shows much faster crystallization compared to the cast films. For 5% *h*-PDLA film, the precrystallized film crystallizes at 137 °C, while the cast film crystallized at 107 °C. It suggests that the thermal history, especially the SC formation process, does affect the overall crystallization rate of PLLA during cooling.

The detailed analysis on the structure of SC crystal in the molten state of PLLA is now necessary to discuss the origin of the acceleration effect of PLLA crystallization. We are going to show in the next section the crystal structure, crystallinity, and viscoelastic properties of SC crystallites.

3.2. Crystal Structure and Viscoelastic Properties of PLLA/PDLA Blends in the Molten State of PLLA Homopolymer. The difference in the efficiency for acceleration of PLLA crystallization is originated from the SC structure and/or the higher order structure in PLLA melt. In order to clarify its structure, WAXD analysis was carried out for the samples quenched from 200 °C. The thermal history applied for the blends was exactly same as that we have shown in Figure 1. At this temperature PLLA homopolymer are in the molten state, and only SC crystal exists because of the melting temperature of PLLA homopolymer and SC is ca. 170 and 230 °C, respectively.[11] The unit cell of SC crystal was recently reported by Sawai et al. to be trigonal cell with cell constants of $a = b = 1.50$ nm, $c = 0.823$ nm, $\alpha = \beta = 90°$, and $\gamma = 120°$.[17] The cell is similar but significantly smaller in *c*-axis length than that previously reported by Cartier et al.[9] Figure 4 shows WAXD profiles of PLLA/PDLA blends quenched from 200 °C after precrystallization at 100 °C for 30 min. The diffraction peaks appear at 2θ values of 12°, 21°, and 24°. These peaks are assigned to be of (110), (300)/(030), and (220), respectively.[17] It clearly indicates that both PLLA/*l*-PDLA (a) and PLLA/*h*-PDLA (b) blends contain

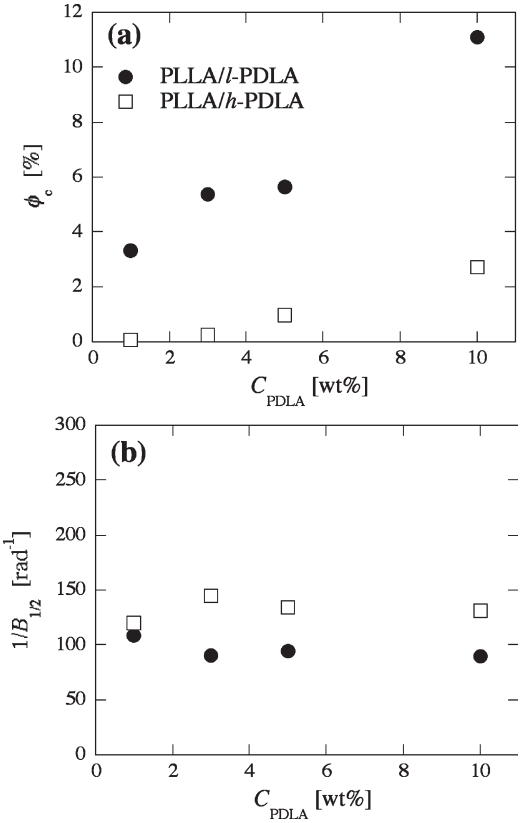

Figure 5. Degree of crystallinity (a) and 1/fwhm (b) of melt-quenched PLLA/PDLA blends plotted as a function of PDLA concentration.

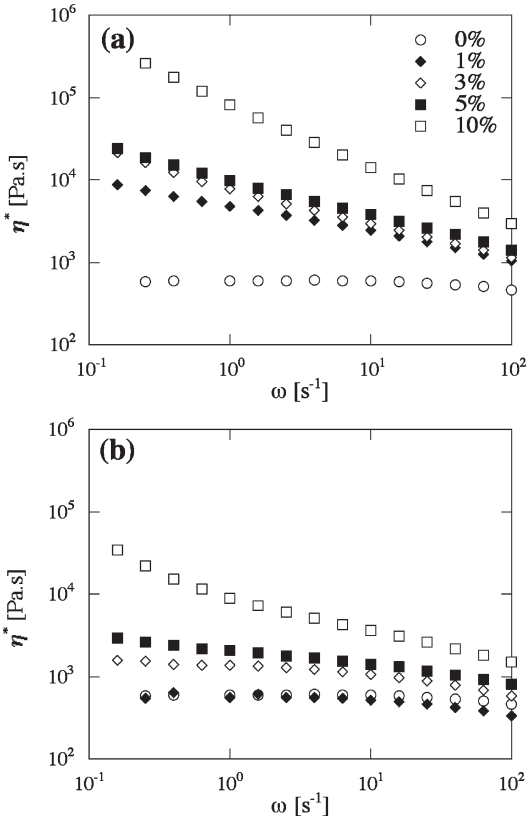

Figure 6. Complex viscosity curves of molten PLLA (200 °C) with various concentrations of *l*-PDLA (a) and *h*-PDLA (b).

SC crystallites at 200 °C. Although the SC exists in the molten state of PLLA homopolymer, the amount of SC seems to depend on the molecular weight of PDLA. In PLLA/*h*-PDLA blend, the diffractions of SC crystal are observed above 3%. No crystal diffraction is observed for 1%, suggesting an absence of SC crystal or more possibly that the crystallinity is too small to detect. For PLLA/*l*-PDLA blends, SC diffractions are observed above the PDLA concentration of 1%. It suggests that the shorter PDLA chains are packed easily into the SC crystal due to its higher mobility. The amount of SC crystal increases with increasing the concentration of PDLA for both blends.

SC crystallinity is estimated from the WAXD profiles shown in Figure 4 over a wide 2θ ranging from 5° to 35° using following equation:

$$\phi_c = \frac{\int_{2\theta=5^\circ}^{2\theta=35^\circ} I_c q^2 \, dq}{\int_{2\theta=5^\circ}^{2\theta=35^\circ} (I_c + I_a) q^2 \, dq}$$

Here, I_c is the diffraction intensity from SC crystal, I_a the amorphous scattering intensity, and q the scattering vector ($q = 4\pi \sin\theta/\lambda$).

The SC crystallinity is plotted in Figure 5a against the concentration of PDLA. It is clearly seen that the SC crystallinity increases monotonously with PDLA concentration. Moreover, the SC crystallinity is always higher in *l*-PDLA blends than that of *h*-PDLA blends.

Figure 5b shows the full width value at half-maximum (fwhm) of (110) plane of the SC crystal for the sample with various PDLA concentrations. It is very important to note that the fwhm stays constant regardless of the PDLA molecular weight or the concentration. It implies that the lateral size of SC crystallites along [110] direction is essentially the same for all samples.

The above finding leads to the question why and how SC crystal accelerate the crystallization of PLLA during cooling. It has been found from Figure 1 that the *h*-PDLA blends are much effective to enhance PLLA crystallization. However, the amount of SC crystal (i.e., crystallinity) was found to be less in *h*-PDLA blends than in *l*-PDLA blends. Since the lateral size of SC crystal is independent of both PDLA molecular weight and the concentration (Figure 5b), the number of the SC crystallites should increase with increasing concentration, when we assume that the crystal thickness is constant because of the same crystallization temperature from glassy state. It is thus reasonable that the acceleration effect of PDLA is not governed by the number density of SC crystallites.

The dynamic oscillatory shear measurement was performed on pure PLLA and PLLA/PDLA blends at 200 °C to investigate the viscoelastic behavior of the molten state of PLLA with SC crystallites. Figure 6 shows the frequency dependences of complex viscosity, η^*, for PLLA/PDLA blends with various PDLA concentrations. The η^* of pure PLLA shows small frequency dependences, revealing a Newtonian plateau in the low-frequency region. However, the η^* increases drastically above the concentration of 1% in PLLA/*l*-PDLA and 3% for PLLA/*h*-PDLA. By the addition of 1% *l*-PDLA, the η^* increases more than one digit in the low-frequency range. The critical concentrations of 1% for *l*-PDLA and 3% for *h*-PDLA are well corresponding to the concentration which shows SC diffraction as seen in Figure 4. The increase in η^* is more pronounced in *l*-PDLA blends than *h*-PDLA blends. It is well agreed with the difference in SC crystallinity shown in Figure 5. These results clearly indicate that the η^* is due to the existence of SC crystallite. However, this increase in η^* seems to be too huge when one reminds that the crystallinity of SC was in the range of

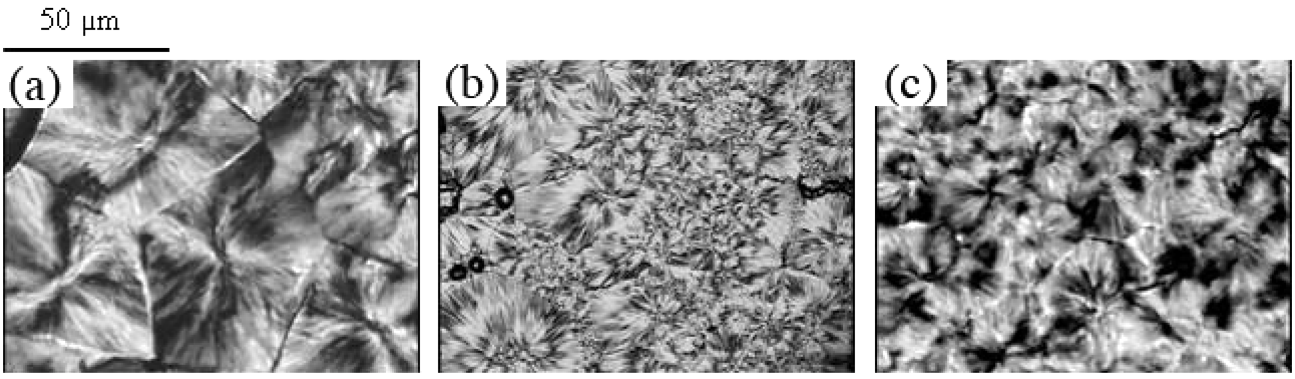

Figure 7. Polarized optical micrographs of PLLA with different concentrations of PDLA at 140 °C after completion of PLLA crystallization: (a) PLLA, (b) PLLA/*l*-PDLA (3%), and (c) PLLA/*h*-PDLA (3%).

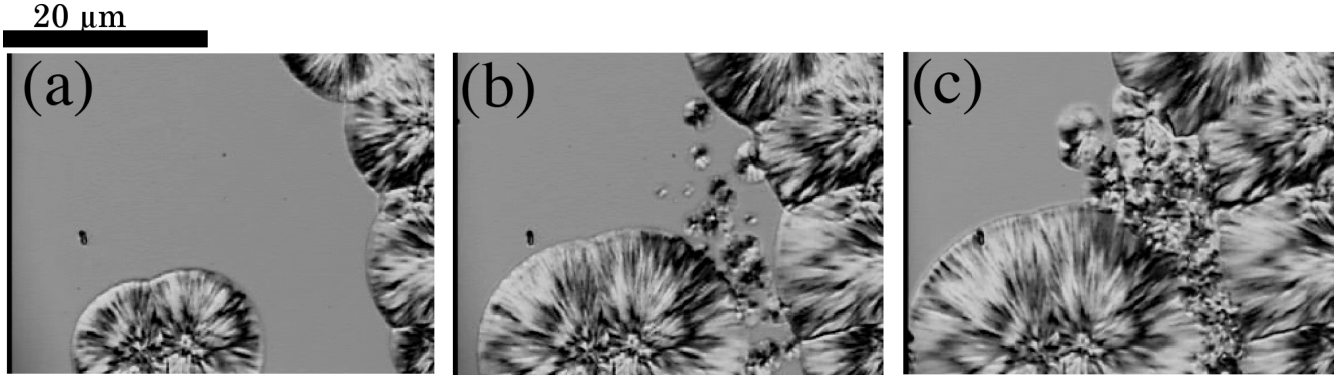

Figure 8. Polarized optical micrographs of PLLA/*l*-PDLA (3%) blend taken at various elapsed times during isothermal crystallization at 140 °C from the melt (200 °C): (a) 50, (b) 70, and (c) 80 min.

several percent (Figure 5). In addition, no plateau region is observed above 1 and 3% for *l*-PDLA and *h*-PDLA in Figure 6. In conventional filled polymer systems, the disappearance of the Newtonian plateau at low frequencies is caused by the strong interaction between filler and the polymer, as reported in PLA/organoclay nanocomposites.[34−36] It suggests that the anomalous rise in η^* comes not only from the SC crystallites as a filler but also from the strong interaction between SC crystallites and/or SC crystallites and PLLA

It is well-known that the melt viscosity strongly depends on its molecular weight. The zero shear viscosity is related to the molecular weight, M, as $\eta_0 = KM^a$, where $a = 3.4$ for a linear polymer with entanglement ($M > M_c$, M_c as the critical molecular weight for the entanglement). Yamane et al. reported that stereocomplex formed from PLLA/PDLA blend acts as a cross-linking point of PLLA chains resulting in the apparent increase in molecular weight.[37] Our results are also reasonably explained by the model that increases in apparent molecular weight, which is originated from the cross-linking of SC crystallites, introduces the excess increase in its viscosity.

3.3. Isothermal Crystallization Behavior. Isothermal crystallization behavior of pure PLLA and PLLA/PDLA blends, especially for the crystallization kinetics, is studied by means of optical microscope. Figure 7 shows the spherulite morphology of (a) PLLA homopolymer, (b) PLLA/*l*-PDLA 3%, and (c) PLLA/*h*-PDLA 3% after isothermal crystallization at 140 °C.

In the previous work, we have shown that the crystal form of PLLA is strongly dependent on the crystallization temperature.[38] Above 120 °C the ordered type α-form is crystallized. In α-form, it is considered that two chains with 10_3 helical conformation are packed into an orthorhombic unit cell with dimension of $a = 10.7$ Å, $b = 6.45$ Å, and c(fiber axis) $= 27.8$ Å.[6] Thus, the spherulite morphologies seen in Figure 7 are of α-form PLLA. Large spherulites, sized about 60 μm in diameter, are seen in PLLA while smaller spherulites are in PDLA blends. In *h*-PDLA blends (Figure 7c), small spherulites with ca. 30 μm in diameter are formed. The spherulites seem to be uniform in size. Considering that the SC crystallites accelerate the crystallization of PLLA during cooling, it suggests that the spatial distribution of SC is uniform in micrometer scale in the PLLA/*h*-PDLA blend. On the other hand, the *l*-PDLA blend shows a different morphology, where the large spherulites sized ca. 50 μm and small with several micrometers coexist in the sample. It may indicate that two different structures exist in the molten state of PLLA, possibly due to the inhomogeneous distribution of SC crystallites in PLLA/*l*-PDLA blends.

Figure 8 shows the time development of PLLA spherulite in 3% *l*-PDLA blend during isothermal crystallization at 140 °C. At the early stage of crystallization, development of large spherulites is observed, followed by the additional nucleation takes place after 70 min. Since the growth rates of large and small spherulites were found to be identical, the size distribution might be due to the difference in nucleation rate.

The effect of the addition of PDLA on crystallization behavior has demonstrated in Figure 9 where the radius of spherulites is plotted against time. Here, we measured the radius growth rate (G) and the induction time (t_i) for PLLA homopolymer spherulite formation. G was estimated from the slope of spherulite radius plotted as a function of crystallization time (t_c), while t_i was evaluated from extrapolation of the spherulite radius line plotted as a function of t_c to a

radius of 0 μm. The rate of nucleation, N, was defined as an inverse of t_i ($N = 1/t_i$).

Effects of the addition of PDLA on the growth rate, G, and the nucleation rate, N, of PLLA during isothermal crystallization at 140 °C are shown in parts a and b of Figure 10, respectively.

The general expression for the growth rate of a linear polymer crystal with folded chain is given by

$$G = G_0 \exp\left[\frac{-U^*}{R(T_c - T_\infty)}\right] \exp\left[\frac{-K_g}{T_c \Delta T f}\right]$$

where K_g is the nucleation constant, ΔT is the degree of undercooling defined by $T_m^\circ - T_c$, T_m° is the equilibrium melting point, f is a factor given as $2T_c/(T_m^\circ + T_c)$, U^* is the activation energy for segment diffusion to the site of crystallization, R is the gas constant, T_∞ is the hypothetical temperature where all motions associated with viscous flow cease ($\sim T_g - 30$ K), and G_0 is the front factor. For PLLA/PDLA blends, no further SC crystal is formed during the isothermal crystallization at 140 °C. Only PLLA or PDLA homocrystal can be formed at this temperature.

Obviously, the growth rate shows a decrease with increasing PDLA concentration regardless the molecular weight of PDLA. We first try to explain above result by the simple model that each SC crystallite is in isolation and acts as a nucleation agent. Since only PLLA lamellae grows into the melt, the PDLA chain must be excluded from the growing front of PLLA lamellae. With increasing the PDLA concentration, the PDLA chains that are not included in SC crystal would increase in the molten state, resulting in the fall in G during crystallization. The decline in G, thus, must be larger in h-PDLA blends because of its lower mobility. Moreover, since SC crystallinity is lower in h-PDLA blends as shown in Figure 5a, there are more "amorphous" PDLA chains in h-PDLA blends, which would interrupt the crystal growth of PLLA.

However, it is interesting to note that the decrease in G is remarkable in l-PDLA blends. It implies that the apparent molecular weight for l-PDLA blends is higher than h-PDLA. This result excludes an idea that the SC crystallites are isolated and gives us the strong evidence that the SC crystallites forms network structure in the molten state of PLLA. Shorter cross-link introduced by l-PDLA is more likely to interrupt the crystal growth of PLLA because of its extremely low mobility. The heterogeneity of the spherulite size in Figure 7 might be due to that of cross-link length, which was originated in the difference in molecular weight between PLLA and PDLA.

The above discussions were made mainly to investigate the difference in the melt structure of PLLA with various concentrations of PDLA. As we described in this article, PDLA/PLLA asymmetric blends have a different acceleration effect on PLLA crystallization according to the concentration and molecular weight of PDLA as well as the sample preparation method (history for the SC formation). However, the crystallization mechanism under existence of SC crystallites and/or network is not yet fully discussed. Since the overall crystallization rate is the product of the nucleation rate by the growth rate, we examine the nucleation rate of PLLA during the isothermal annealing.

The concentration dependence of the nucleation rate of PLLA is shown in Figure 10b. It is clearly seen that the nucleation rate is also influenced by the PDLA concentration. Interestingly, it shows the different concentration dependence according to the molecular weight of PDLA. For h-PDLA blend, increase in N is monotonous. N rises more than 1 digit by adding 10% h-PDLA, while a peculiar concentration dependence was seen for l-PDLA. N increases up to 1%, followed by leveling off at higher concentration. It should be mentioned that the concentration dependence in N follows the same trend as that in overall crystallization rate, which we have shown in Figure 2. It implies that the acceleration effect of SC crystallite in PDLA/PLLA blend is originated in the enhancement in the nucleation process.

The nucleation rate I^* can be expressed as the following equation[39]

$$I = I_0 \exp\left(-\frac{U^*}{kT_c}\right) \exp\left(-\frac{\Delta G^*}{kT_c}\right)$$

where k and I_0 are the Boltzmann constant and a prefactor, respectively. U^* and ΔG^* are the activation energy for

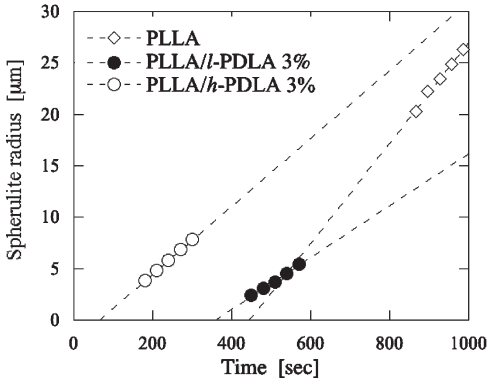

Figure 9. Change in the radius of PLLA spherulite during isothermal crystallization at 140 °C.

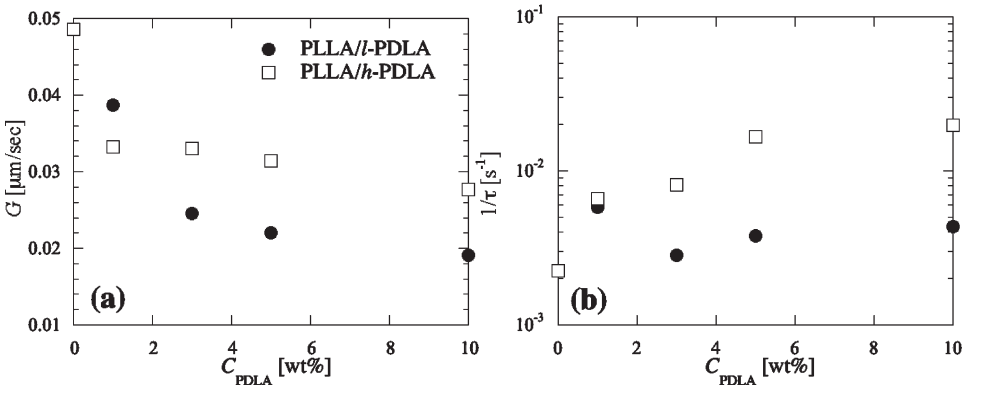

Figure 10. Growth rate G (a) and nucleation rate N (b) of PLLA spherulite during crystallization at 140 °C plotted as a function of PDLA.

diffusion and the energy barrier for the formation of critical nucleus, respectively. It is well-known that the nucleating agent offers a specific surface for heterogeneous nucleation of polymers, mostly via epitaxial relationship among them,[40] resulting in the reduction of ΔG^*. In this case, the nucleating agent has no influence on the growth rate of polymer. Okada et al. have reported that the induction time of nucleation does not depend on the concentration of the nucleating agent.[41] The acceleration of polymer crystallization is, thus, achieved by the increases in the nucleation site for polymer spherulite by adding the nucleating agent.

Our results shown in this article cannot be explained simply by the "nucleating agent model" proposed by several authors,[20,21,32] where PLLA with 10_3 helical structure nucleates on the SC with 3_1 helix, although the model might be partly involved in this acceleration effect.

The above discussion leads us to propose the acceleration mechanism as follows. In PLLA/*h*-PDLA blends, the network structure develops uniformly as the SC crystallinity increases. This network structure slightly interrupts the crystal growth of PLLA during cooling and/or isothermal annealing but brings sharp increase in nucleation process. Why can the network structure accelerate the nucleation process? We believe that the local stress in the supercooled melt plays an important role for the acceleration. When polymer is subjected to the temperature jump from the molten state, large thermal shrinkage takes place prior to the crystallization, resulting in the local stress in supercooled melt. In the PLLA/PDLA system, PLLA chains in the molten state are confined to the network structure. Since this local stress would be more pronounced in the network system, one can expect the reduction of ΔG^* due to the conformational entropy loss. The acceleration effect of PLLA crystallization in PLLA/*h*-PDLA, thus, arises from stress-induced nucleation due to the existence of the homogeneously distributed SC network.

While in PLLA/*l*-PDLA, a steady increase in overall crystallization rate is abandoned above 3% due to the inhomogeneous spatial distribution of SC. It might be related to the difference in chain length that forms network structure in the molten state of PLLA. As the number of shorter cross-link increases with the concentration, the obstruction of PLLA crystal growth is more pronounced in PLLA/*l*-PDLA blends. The delay in nucleation at higher concentration is complex. The cohesion of SC crystallites might be a reason for this peculiar concentration dependence in PLLA/*l*-PDLA blends as seen in Figure 8.

4. Conclusion

The effect of the addition of PDLA on the crystallization behavior of PLLA was investigated. Nonisothermal and isothermal crystallization behaviors of PLLA in addition of low (*l*-PDLA) and high molecular weight PDLA (*h*-PDLA) were studied. PLLA/PDLA asymmetric blends formed stereocomplex crystallites and stay unmelted at 200 °C in the PLLA melt region. Nonisothermal crystallization measurement from 200 °C showed a monotonous rise in the crystallization temperature for PLLA/*h*-PDLA blends, while a peculiar concentration dependence was observed for PLLA/*l*-PDLA blends. The acceleration effect was more pronounced in PLLA/*h*-PDLA blends, which implies the importance of higher order structure of SC. From isothermal crystallization kinetics measurements, the acceleration effect in PLLA/PDLA blend was found to enhance the nucleation of crystallization but slightly interrupt the crystallization growth. The above results were reasonably explained by the model where SC crystallites are not isolated in PLLA melt but connected like a physical gel.

References and Notes

(1) Garlotta, D. *J. Environ. Polym. Degrad.* **2001**, *9*, 63.
(2) Nam, J. Y.; Okamoto, M.; Okamoto, H.; Nakano, M.; Usuki, A.; Matsda, M. *Polymer* **2006**, *47*, 1340.
(3) Miyata, T.; Masuko, T. *Polymer* **1997**, *38*, 4003.
(4) De Santis, P.; Kovacs, A. J. *Biopolymer* **1968**, *6*, 299.
(5) Hoogsteen, W.; Postema, A. R.; Pennings, A. J.; ten Brinke, G.; Zugenmaier, P. *Macromolecules* **1990**, *23*, 634.
(6) Kobayashi, J.; Asahi, T.; Ichiki, M.; Okikawa, A.; Suzuki, H.; Watanabe, T.; Fukuda, E.; Shikinami, Y. *J. Appl. Phys.* **1995**, *77*, 2957.
(7) Sasaki, S.; Asakura, T. *Macromolecules* **2003**, *36*, 8385.
(8) Brizzolara, D.; Cantow, H. J.; Diederichs, K.; Keller, E.; Domb, A. J. *Macromolecules* **1996**, *29*, 191.
(9) Cartier, L.; Okihara, T.; Ikada, Y.; Tsuji, H.; Puiggali, J.; Lotz, B. *Polymer* **2000**, *41*, 8909.
(10) Puiggali, J.; Ikada, Y.; Tsuji, H.; Cartier, L.; Okihara, T.; Lotz, B. *Polymer* **2000**, *41*, 8921.
(11) Ikada, Y.; Jamshidi, K.; Tsuji, H.; Hyon, S.-H. *Macromolecules* **1987**, *20*, 3.
(12) Slager, J.; Jamshidi, K.; Tsuji, H.; Hyon, S.-H. *Macromolecules* **1987**, *20*, 904.
(13) Tsuji, H. *Macromol. Biosci.* **2005**, *5*, 569.
(14) Tsuji, H.; Ikada, Y. *Polymer* **1999**, *40*, 6699.
(15) Tsuji, H.; Fukui, I. *Polymer* **2003**, *44*, 2891.
(16) Okihara, T.; Tsuji, M.; Kawaguchi, A.; Katayama, K. *J. Macromol. Sci., Phys.* **1991**, *B30*, 119.
(17) Sawai, D.; Tsugane, Y.; Tamada, M.; Kanamoto, T.; Sungil, M.; Hyon, S.-H. *J. Polym. Sci., Part B: Polym. Phys.* **2007**, *45*, 2632.
(18) Kolstad, J. J. *J. Appl. Polym. Sci.* **1996**, *62*, 1079.
(19) Haubruge, H. G.; Daussin, R.; Jonas, A. M.; Legras, R. *Macromolecules* **2003**, *36*, 5.
(20) Schmidt, S. C.; Hillmyer, M. A. *J. Polym. Sci., Part B: Polym. Phys.* **2001**, *39*, 300.
(21) Yamane, H.; Sasai, K. *Polymer* **2003**, *44*, 2569.
(22) Anderson, K. S.; Hillmeyer, M. A. *Polymer* **2006**, *47*, 2030.
(23) Tsuji, H.; Takai, H.; Saha, S. K. *Polymer* **2006**, *47*, 3826.
(24) Tsuji, H.; Horii, F.; Hyon, S.-H.; Ikada, Y. *Macromolecules* **1991**, *24*, 2719.
(25) Tsuji, H.; Hyon, S.-H.; Ikada, Y. *Macromolecules* **1991**, *24*, 5651.
(26) Tsuji, H.; Hyon, S.-H.; Ikada, Y. *Macromolecules* **1991**, *24*, 5657.
(27) Tsuji, H.; Hyon, S.-H.; Ikada, Y. *Macromolecules* **1992**, *25*, 2940.
(28) Tsuji, H.; Horii, F.; Nakagawa, M.; Ikada, Y.; Odani, H.; Kitamaru, R. *Macromolecules* **1992**, *25*, 4114.
(29) Tsuji, H.; Ikada, Y. *Macromolecules* **1992**, *25*, 5719.
(30) Tsuji, H.; Ikada, Y. *Macromolecules* **1993**, *26*, 6918.
(31) Tsuji, H.; Ikada, Y. *J. Appl. Polym. Sci.* **1994**, *53*, 1061.
(32) Brochu, S.; Prud'homme, R. E.; Barakat, I.; Jerome, R. *Macromolecules* **1995**, *28*, 5230.
(33) Tsuji, H. *Macromol. Chem. Phys.* **1996**, *197*, 3483.
(34) Hoffman, B.; Dietrich, C.; Thomann, R.; Freidrich, C.; Mulhaupt, R. *Macromol. Rapid Commun.* **2000**, *21*, 57.
(35) Ray, S. S.; Okamoto, M. *Prog. Polym. Sci.* **2003**, *28*, 1539.
(36) Di, Y.; Iannace, S.; Maio, E. D.; Nicolais, L. *J. Polym. Sci., Part B: Polym. Phys.* **2005**, *43*, 689.
(37) Yamane, H.; Sasai, K.; Takano, M. *J. Rheol.* **2004**, *48*, 599.
(38) Kawai, T.; Rahman, N.; Matsuba, G.; Nishida, K.; Kanaya, T.; Nakano, M.; Okamoto, H.; Kawada, J.; Usuki, A.; Honma, N.; Nakajima, K.; Matsuda, M. *Macromolecules* **2007**, *40*, 9463.
(39) Wunderlich, B. *Macromolecular Physics*; Academic Press: New York, 1976; Vol. 2.
(40) Kawai, T.; Iijima, R.; Yamamoto, Y.; Kimura, T. *Polymer* **2002**, *43*, 7301.
(41) Okada, K.; Watanabe, K.; Urushihara, T.; Toda, A.; Hikosa, M. *Polymer* **2007**, *48*, 401.